Monthly Notices
of the
ROYAL ASTRONOMICAL SOCIETY

Mon. Not. R. Astron. Soc. **411,** 1204–1212 (2011) doi:10.1111/j.1365-2966.2010.17753.x

Transit timing variation and activity in the WASP-10 planetary system⋆

G. Maciejewski,[1,2]† D. Dimitrov,[3] R. Neuhäuser,[1] N. Tetzlaff,[1] A. Niedzielski,[2] St. Raetz,[1] W. P. Chen,[4] F. Walter,[5] C. Marka,[1] S. Baar,[1] T. Krejcová,[6] J. Budaj,[7] V. Krushevska,[7,8] K. Tachihara,[9] H. Takahashi[10] and M. Mugrauer[1]

[1]*Astrophysikalisches Institut und Universitäts-Sternwarte, Schillergässchen 2–3, D-07745 Jena, Germany*
[2]*Toruń Centre for Astronomy, N. Copernicus University, Gagarina 11, PL-87100 Toruń, Poland*
[3]*Institute of Astronomy, Bulgarian Academy of Sciences, 72 Tsarigradsko Chausse Blvd, 1784 Sofia, Bulgaria*
[4]*Institute of Astronomy, National Central University, 300 Jhongda Rd, Jhongli 32001, Taiwan*
[5]*Department of Physics and Astronomy, SUNY, Stony Brook, NY 11794-3800, USA*
[6]*Masaryk University, Department of Theoretical Physics and Astrophysics, 602 00 Brno, Czech Republic*
[7]*Astronomical Institute of the Slovak Academy of Sciences, 059 60 Tatranská Lomnica, Slovak Republic*
[8]*Main Astronomical Observatory of National Academy of Sciences of Ukraine, 27 Akademika Zabolotnoho St, 03680 Kyiv, Ukraine*
[9]*National Astronomical Observatory of Japan, ALMA project office, 2-21-1 Osawa Mitaka, Tokyo 181-8588, Japan*
[10]*Gunma Astronomical Observatory, 6860-86 Nakayama, Takayama-mura, Agatsuma-gun, Gunma 377-0702, Japan*

Accepted 2010 September 22. Received 2010 September 22; in original form 2010 July 16

ABSTRACT

Transit timing analysis may be an effective method of discovering additional bodies in extra-solar systems that harbour transiting exoplanets. The deviations from the Keplerian motion, caused by mutual gravitational interactions between planets, are expected to generate transit timing variations of transiting exoplanets. In 2009, we collected nine light curves of eight transits of the exoplanet WASP-10b. Combining these data with those published, we have found that transit timing cannot be explained by a constant period but by a periodic variation. Simplified three-body models, which reproduce the observed variations of timing residuals, were identified by numerical simulations. We have found that the configuration with an additional planet with a mass of $\sim$0.1 M_J and an orbital period of $\sim$5.23 d, located close to the outer 5 : 3 mean motion resonance, is the most likely scenario. If the second planet is a transiter, the estimated flux drop will be $\sim$0.3 per cent and can be observed with a ground-based telescope. Moreover, we present evidence that the spots on the stellar surface and the rotation of the star affect the radial-velocity curve, giving rise to a spurious eccentricity of the orbit of the first planet. We argue that the orbit of WASP-10b is essentially circular. Using the gyrochronology method, the host star was found to be 270 ± 80 Myr old. This young age can explain the large radius reported for WASP-10b.

Key words: planets and satellites: individual: WASP-10b – stars: individual: WASP-10.

1 INTRODUCTION

The analysis of transit timing variations (TTVs) of exoplanets is expected to be an efficient method for discovering additional low-mass planets (Miralda-Escudé 2002; Schneider 2004; Holman & Murray 2005; Agol et al. 2005; Steffen et al. 2007). Many studies have been performed to detect TTV signals but these have resulted only in constraints on the parameters of hypothetical second planets (e.g. Gibson et al. 2009). Recently, Maciejewski et al. (2010) have detected a variation in the transit timing of WASP-3b. They have found that a configuration with a hypothetical second planet with a mass of $\sim 15\,M_\oplus$, located close to an outer 2 : 1 mean motion resonance (MMR), may reproduce the observed TTV signal. Lendl et al. (2010) have found some indications for the TTV for OGLE2-TR-L9b, but no preliminary solution has been proposed.

WASP-10b is an exoplanet, which was discovered by Christian et al. (2009). The mass and radius of the planet have been found to be $2.96^{+0.22}_{-0.17}\,M_J$ and $1.28^{+0.08}_{-0.09}\,R_J$, respectively, larger than the interior models of irradiated giant planets predict. The planet orbits its host star in $\sim$3.09 d at an orbital semimajor axis of $0.0369^{+0.0012}_{-0.0014}$ au. The

⋆Partly based on observations made with the 0.6- and 2.0-m telescopes of the Rozhen National Astronomical Observatory, which is operated by the Institute of Astronomy, Bulgarian Academy of Sciences, and the 90-cm telescope of the University Observatory Jena, which is operated by the Astrophysical Institute of the Friedrich Schiller University.

†E-mail: gm@astro.uni-jena.de

eccentricity of the orbit has been reported to be $0.059^{+0.014}_{-0.004}$ – a large value for a close-in planet. In the paper reporting on its discovery, Christian et al. (2009) determined the transit depth and duration to be 29 mmag and 2.36 h, respectively.

Johnson et al. (2009, 2010) have redetermined the planet's parameters with a high-precision light curve using the 2.2-m telescope of the University of Hawaii with a photometric precision of 4.7×10^{-4} and a mid-transit time error of 7 s. The mass of the planet has been found to be $3.15^{+0.13}_{-0.11}\,M_J$ and the planetary radius has turned out to be noticeably smaller (i.e. $1.08 \pm 0.02\,R_J$). The latter result has not been confirmed by the studies of Krejcová, Budaj & Krushevska (2010) or Dittmann et al. (2010). The first team have found the radius of WASP-10b to be in excellent agreement with the value obtained by Christian et al. (2009), and a similar conclusion has been reached by Dittmann et al. (2010) with no TTV signature detected.

The host star ($V = 12.7$ mag) is a K5 dwarf with an effective temperature of 4675 ± 100 K, located 90 ± 20 pc from the Sun (Christian et al. 2009). Smith et al. (2009) have confirmed the previous evidence that the light curve of WASP-10 exhibits a rotational photometric variability caused by star-spots. The stellar rotation period has been found to be 11.91 ± 0.05 d, in agreement with ∼12 d reported by Christian et al. (2009).

It has been suggested that the presence of an additional small planet could pump the eccentricity of WASP-10b (Christian et al. 2009). This system is therefore a good target for TTV studies.

The order of this paper is as follows. In Section 2, we summarize observations and data reduction. We present the discovery of the periodic TTV in Section 3. We describe the process of identifying and verifying the most likely two-planetary model of the WASP-10 system in Section 4. We present a discussion of the proposed scenario in Section 5. Finally, we give our conclusions in Section 6.

2 OBSERVATIONS AND DATA REDUCTION

We have collected nine light curves of eight transits of WASP-10b during a dedicated international observing campaign involving telescopes worldwide at different longitudes (listed in Tables 1 and 2). The transit on 2009 July 31 was observed with two instruments in different observatories. The telescope diameters of 0.6–2.0 m allowed us to collect photometric data with 1.1–2.7 mmag precision. Observations generally started ∼1 h before the expected beginning of a transit and ended ∼1 h after the event. However, weather conditions and schedule constraints meant that we were not always able to follow this scheme.

Table 2. The summary of observing runs. ID is the identification of the instrument according to Table 1, N_{exp} is the number of useful exposures, T_{exp} is the exposure time. Dates (UT) are given for the beginning of the night.

Run	Date	ID	Filter	N_{exp}	T_{exp} (s)
1	2009 Jan. 5	1	*R*	254	50
2	2009 Jul. 31	2	*R*	144	60, 80
3	2009 Jul. 31	3	*R*	116	120
4	2009 Aug. 3	3	*R*	122	90
5	2009 Aug. 28	3	*R*	99	90
6	2009 Aug. 31	2	*R*	203	50, 60
7	2009 Sep. 3	3	*R*	105	90
8	2009 Oct. 1	4	*V*	548	15
9	2009 Nov. 17	5	*R*	76	90

Standard IDL procedures (adapted from DAOPHOT) were used for the reduction of the photometric data collected at the National Astronomical Observatory at Rozhen, Bulgaria, and for computing the differential aperture photometry. Using the method of Everett & Howell (2001), several stars (four to six) with photometric precision better than 5 mmag were selected to create an artificial standard star used for differential photometry. Data from the remaining telescopes were reduced with the software pipeline developed for the Semi-Automatic Variability Search sky survey (Niedzielski, Maciejewski & Czart 2003). To generate an artificial comparison star, 30–50 per cent of the stars with the lowest light-curve scatter were selected iteratively from the field stars brighter than 3 mag below the saturation level. To measure instrumental magnitudes, various aperture radii were used. The aperture that was found to produce light curves with the smallest scatter was used to generate a final light curve.

3 RESULTS

3.1 Light-curve analysis

A model-fitting algorithm available via the Exoplanet Transit Data base (Poddaný, Brát & Pejcha 2010) was used to derive transit parameters: duration, depth and mid-transit time. The procedure employs the OCCULTSMALL routine of Mandel & Agol (2002) and the

Table 1. A list of the telescopes. FOV is the field of view of the instrument and N_{tr} is the number of observed transits.

ID	Telescope	Observatory and Location	Detector and CCD size	N_{tr} and FOV (arcmin)
1	0.6-m Cassegrain	Astronomical Observatory, N.Copernicus University Piwnice near Toruń, Poland	SBIG STL-1001 1024 × 1024, 24 μm	1 11.8 × 11.8
2	0.6-m Schmidt[a]	University Observatory Jena, Großschwabhausen near Jena, Germany	CCD-imager STK 2048 × 2048, 13.5 μm	2 52.8 × 52.8
3	0.6-m Cassegrain	National Astronomical Observatory Rozhen, Bulgaria	FLI PL09000 3056 × 3056, 12 μm	4 17.3 × 17.3
4	2-m Ritchey-Chrétien	National Astronomical Observatory Rozhen, Bulgaria	PI VersArray:1300B 1340 × 1300, 20 μm	1 5.8 × 5.6
5	0.8-m Tenagra II	Tenagra Observatories Arizona, USA	SITe 1024 × 1024, 24 μm	1 14.8 × 14.8
6	1.5-m Ritchey-Chrétien	Gunma Astronomical Observatory Takayama, Japan	Andor DW432 1250 × 1152, 24 μm	0[b] 12.5 × 11.5

[a] See Mugrauer & Berthold (2010) for details.
[b] No scientific output because of bad weather conditions.

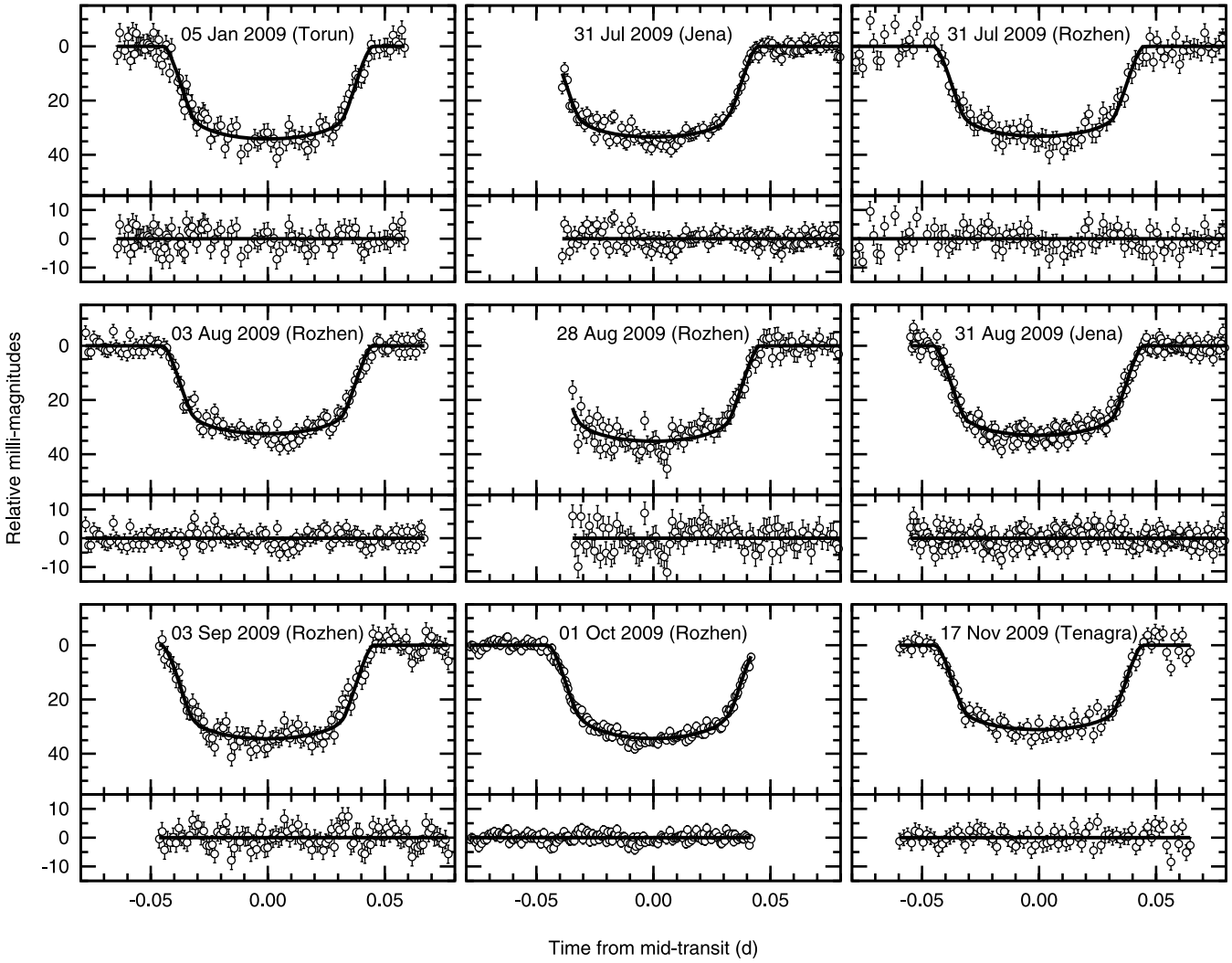

Figure 1. Light curves of WASP-10b transits in individual runs. The best-fitting models are shown as solid lines. The transit on July 31 was observed simultaneously by two observatories.

Levenberg–Marquardt non-linear least-squares fitting algorithm, which also provides uncertainties. As our research was focused on determining mid-transit times, the number of parameters to be fitted could be reduced. An impact parameter $b = a \cos i/R_* = 0.299^{+0.029}_{-0.043}$ (where a is the semimajor axis, i is the inclination and R_* is the host–star radius) was taken from Johnson et al. (2009) and was fixed during the fitting procedure. We used the linear limb-darkening law of Van Hamme (1993) with the limb-darkening coefficient linearly interpolated for the host star in a given filter. A first- or second-order polynomial was used to remove trends in magnitude or flux. The mid-transit times were corrected from UTC to Terrestrial Dynamical Time (TT) and then transformed into the Barycentric Julian Date (BJD) (Eastman, Siverd & Gaudi 2010). Light curves with best-fitting models and residuals are shown in Fig. 1 and the derived parameters are given in Table 3.

Krejcová et al. (2010) have also published observations and R-band light curves of four complete transit events of WASP-10b. In their analysis, they have focused mainly on the determination of the planet radius and have not studied the mid-transit times, the O − C diagram or TTVs. We determine four mid-transit times for these observations and place them into the context of our data to create a larger sample for TTV analysis. We have used the same method to determine the mid-transit times from their light curves as for all other observations presented here. The corresponding mid-transit times are presented in Table 3.

Across all data sets, two transits on epochs 222 and 232 were observed simultaneously by two different telescopes. The data were reduced with different pipelines and by different teams. The transit on epoch 222 was observed with the 60-cm telescopes in Jena and at Rozhen. The difference in mid-transit times was found to be ∼11 s. The transit on epoch 232 was covered by observations in Jena and by the 50-cm telescope in Stará Lesná in Slovakia (Krejcová et al. 2010). In this case, the discrepancy of timing was found to be ∼18 s. Timing differences are well within the error bars of individual determinations for both transits. This practical test strengthens the reliability of our mid-transit time determinations.

3.2 Detection of a transit timing variation

While determining new linear ephemeris, we noted that a linear fit of the epoch E and orbital period P_b of WASP-10b resulted in reduced $\chi^2_{red} = 13.8$. Individual mid-transit errors were taken as weights in the fitting procedure. Such a high value of χ^2_{red} suggests the existence of an additional signal in the O − C diagram (Fig. 2).

Table 3. Parameters of transit light-curve modelling. T_0 denotes the mid-transit time, T_d is the transit time duration, δ is the depth, σ is the averaged standard deviation of the fit and E is the epoch. The O − C values have been calculated according to the linear part of equation (1) and the best-fitting parameters. The O − C values are given both in days and in uncertainties of the mid-transit times. t_{cad} is the mean cadence of a light curve. The results of reanalysed data from Krejcová et al. (2010) are collected below the horizontal line. BJD times are based on TT.

Run	T_0 $BJD_{TT} - 245\,0000$	T_d (min)	δ (mmag)	σ (mmag)	E	O − C (d)	O − C (T_0 errors)	t_{cad} (s)
1	4837.23116 ± 0.00037	128.9 ± 1.4	34.1 ± 0.8	2.7	155	−0.00030	−0.8	56
2	5044.44427 ± 0.00032	128.9 ± 1.2	33.5 ± 1.1	1.7	222	+0.00069	+2.2	87
3	5044.44415 ± 0.00040	129.1 ± 1.5	33.1 ± 0.7	2.6	222	+0.00057	+1.4	130
4	5047.53696 ± 0.00028	129.4 ± 1.0	32.4 ± 0.5	2.0	223	+0.00066	+2.3	103
5	5072.27861 ± 0.00053	131.1 ± 2.1	35.2 ± 0.8	2.5	231	+0.00056	+1.1	102
6	5075.37129 ± 0.00024	129.2 ± 0.8	33.0 ± 0.7	2.0	232	+0.00053	+2.2	63
7	5078.46485 ± 0.00044	130.4 ± 1.5	34.5 ± 1.1	2.5	233	+0.00137	+3.1	102
8	5106.29681 ± 0.00021	129.8 ± 0.7	34.4 ± 0.7	1.1	242	−0.00115	−5.4	19
9	5152.68923 ± 0.00039	128.8 ± 1.3	33.3 ± 2.4	2.1	257	+0.00051	+1.3	143
	4775.37834 ± 0.00042				135	+0.00125	+2.9	35
	5075.37150 ± 0.00034				232	+0.00073	+2.2	26
	5109.39135 ± 0.00052				243	+0.00068	+1.3	36
	5112.48528 ± 0.00035				244	+0.00189	+5.4	36

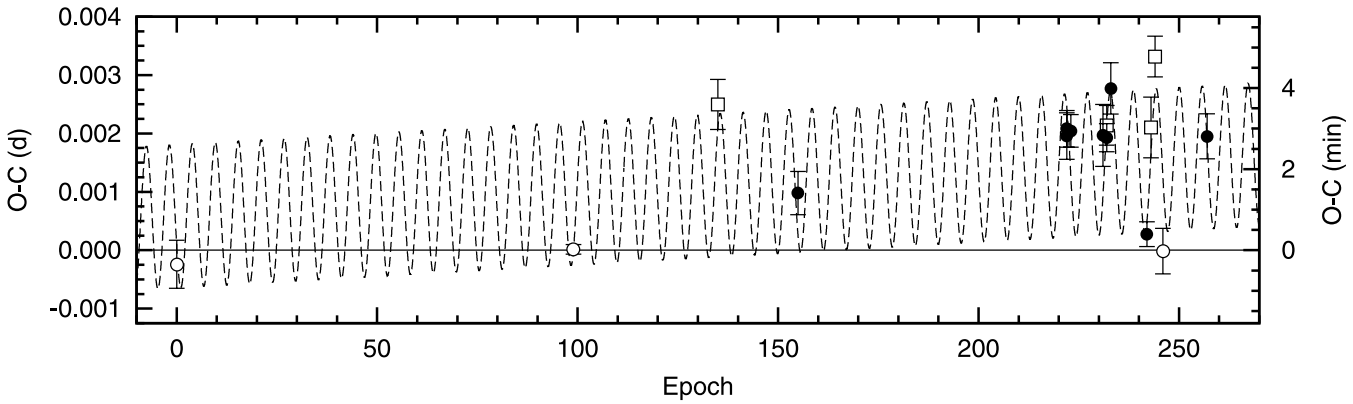

Figure 2. The observation minus calculation (O − C) diagram for WASP-10b, generated for linear ephemeris based on data from the literature (solid line). Open circles denote the data from the literature, taken from Christian et al. (2009), Johnson et al. (2010) and Dittmann et al. (2010). Open squares are based on reanalysed photometry from Krejcová et al. (2010). Filled symbols denote results from our campaign. A significantly better fit may be obtained for the new ephemeris given by equation (1) (dashed line). The 3σ error bars were taken for the mid-transit time reported by Dittmann et al. (2010). Their light curve was not corrected for a linear trend, which is clearly visible in out-of-transit phases (J. Dittmann, private communication). Our tests have shown that this effect significantly affects the accuracy of the mid-transit time.

The Lomb–Scargle periodogram (Lomb 1976; Scargle 1982) of the residuals reveals the existence of two peaks of similar significance and frequencies of 0.175 and 0.183 cycl P_b^{-1} (Fig. 3). For each frequency, an ephemeris was refitted with the linear trend plus a sinusoidal variation in the form:

$$T_b = T_0 + E\,P_b + A_{ttv}\sin\left(2\pi\frac{E - E_{ttv}}{P^{ttv}}\right) \quad (1)$$

Here, T_0 is the mid-transit time for the initial epoch ($E = 0$), A_{ttv} is the semi-amplitude of the detected TTV, E_{ttv} is the epoch offset of the TTV signal and P^{ttv} is its period. The minimal $\chi^2_{red} = 3.2$ was obtained for $f_1^{ttv} = 0.183$ cycl P_b^{-1} and resulted in $T_0 = 245\,4357.86011 \pm 0.00047$ BJD_{TT}, $P_b = 3.0927183 \pm 0.0000021$ d, $A_{ttv} = 0.00120 \pm 0.00036$ d, $E_{ttv} = 1.8 \pm 0.4$ and $P_1^{ttv} = 5.473 \pm 0.012\ P_b$.

The procedure run for $f_2^{ttv} = 0.175$ cycl P_b^{-1} gave $\chi^2_{red} = 4.1$, $P_2^{ttv} = 5.7172 \pm 0.0082\ P_b$ and similar values of T_0 and P_b. In this case, the fit turned out to be poorer, and thus we used the ephemeris based on parameters obtained for P_1^{ttv}.

The ephemeris calculated according to equation (1) (and P_1^{ttv}) is plotted in Fig. 2 with a dashed line. The O − C values, which are used in further analysis, were calculated according to the linear part of equation (1).

To check if a random distribution of data points in the O − C diagram may favour the detected frequencies, 10^5 fake data sets were generated. The original residuals were replaced with random values with a white-noise distribution of the amplitude. Then, the Lomb–Scargle algorithm was run to find a dominant frequency in each fake diagram. Fig. 4 shows a histogram of these frequencies, with the number of bins equal to the square root of the number of data points in the sample. Detected TTV frequencies, f_1^{ttv} and f_2^{ttv}, are not associated with any significant peak in the histogram.

Kipping & Bakos (2010a) have pointed out that the transit phasing, which is the time difference between the expected mid-transit moment and the nearest data point in a light curve, may generate a spurious TTV signal. For example, for a light curve of 60-s cadence, the time difference is expected to be ±30 s (Kipping & Bakos 2010b). Cadences of our individual light curves are in a wide range between 19 and 143 s (see Table 3) with the median value of

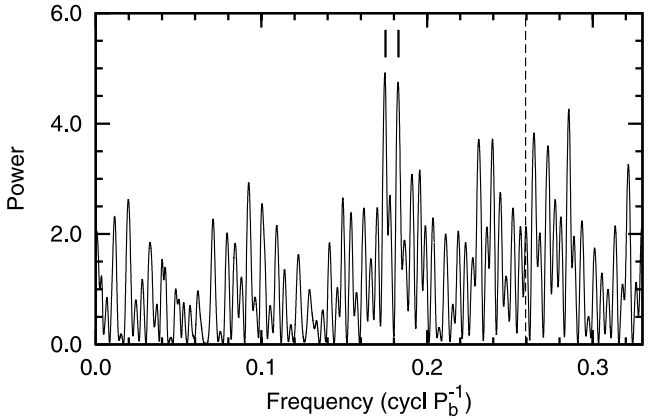

Figure 3. The Lomb–Scargle periodogram generated for the timing residuals plotted in Fig. 2, showing the existence of a periodic signal. The most significant peaks are indicated. The upper limit of the periodogram is determined by the Nyquist frequency for the data set. The vertical dashed line marks the rotational period of the host star (see Section 5).

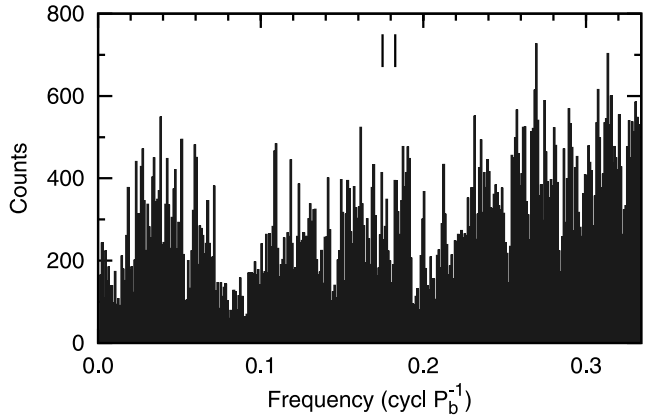

Figure 4. The distribution of dominant frequencies for 10^5 fake O − C diagrams with observed data points replaced by the white noise. The number of bins is equal to the square root of the number of data points in the sample and the width of individual bins is 0.001 cycl P_b^{-1}. Detected TTV frequencies, f_1^{ttv} and f_2^{ttv}, are indicated. No significant peak is associated with any of these, which indicates that a spectral window is not a source of detected periodicities.

63 s. This value is ∼ three times smaller than the amplitude of the detected TTV signal. As shown in Fig. 5, no correlation between individual residuals and cadences was detected. A formal least-squares fit to this data set resulted in the correlation coefficient $R = -0.36$, which clearly reveals no correlation at the relevant level. The checks discussed above strengthen the detection of the TTV signal in our data set.

4 TWO-PLANETARY MODEL

The possible non-zero eccentricity postulated by Christian et al. (2009) might potentially have resulted from confusion with a two-planet system in which both planets orbit their host star in circular orbits in an inner 2 : 1 resonance (Anglada-Escude, López-Morales & Chambers 2010). Although we argue later that the eccentricity of WASP-10b is indistinguishable from zero, the case of an inner

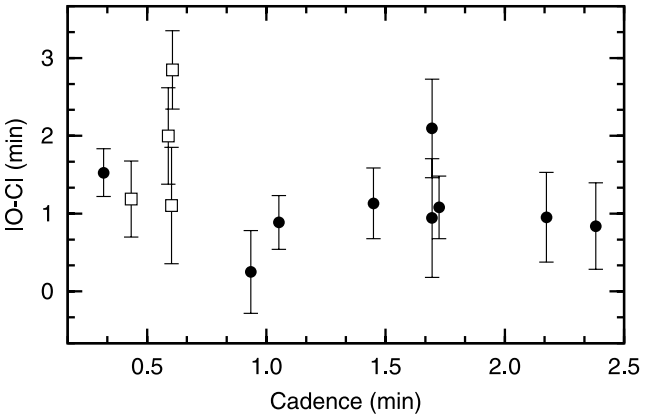

Figure 5. Absolute values of individual residuals in transit timing versus cadence. Symbols denote the same data sets as in Fig. 2. No correlation between both quantities was found.

perturber was considered for the completeness of our analysis.[1] Assuming circular orbits, the mass of the perturbing planet M_c depends on the mass of the outer, more massive transiting planet M_b and its apparent eccentricity e_b (Anglada-Escude et al. 2010). This results in $M_c \approx 0.14\,M_J$ in the WASP-10 system. Such a planet is expected to produce strong gravitational perturbations, which should be visible as the TTVs of WASP-10b. To check this scenario, we have generated synthetic O − C diagrams for WASP-10b in systems with a second planet. Parameters of the transiting planet and its host star were taken from Johnson et al. (2009). Initial circular and coplanar orbits were assumed for both planets. The perturbing planet was put in an orbit with the semimajor axis between 0.0218 and 0.0257 au (±0.0020 au away from the 2 : 1 orbital resonance). Calculations were performed using the MERCURY package (Chambers 1999) employing the Bulirsch–Stoer integrator. Simulations covered 270 periods of WASP-10b (i.e. the time-span covered by observations). No configuration was found to reproduce periodicity close to P_1^{ttv} and P_2^{ttv}. The procedure was repeated for the inner 3 : 1 and 3 : 2 MMRs but these cases also brought negative results.

To search for configurations with an outer perturber reproducing P_1^{ttv} and P_2^{ttv}, synthetic O − C diagrams were generated with the PTMET code, which is based on perturbation theory (Nesvorný & Morbidelli 2008; Nesvorný 2009). Both planets were put in initial circular orbits. The semimajor axis a_c of the perturber varied between 0.0500 and 0.3000 au in steps of 0.0001 and 0.0002 au for $a_c \leq 0.1$ and $a_c > 0.1$ au, respectively. The amplitude of the TTV signal scales nearly linearly with the perturber's mass (Nesvorný & Morbidelli 2008). Thus, M_c was fixed and set equal to $0.3\,M_J$ for the preliminary identification. Each simulation covered 270 periods of WASP-10b. Periodic signals reproducing P_1^{ttv} and P_2^{ttv} were identified close to 5 : 3 and 5 : 2 MMRs for perturber masses of ∼0.1 and ∼$0.5\,M_J$, respectively.

To refine the parameters of a perturbing body, the synthetic O − C diagrams were calculated with the MERCURY code and the Bulirsch–Stoer integrator. The initial parameters of planet c were taken from previous simulations and then refined with the mass varying in steps of $0.05\,M_J$. Each simulation covered 31 000 d (i.e. ∼10 000 periods of WASP-10b). The synthetic O − C diagrams were directly fitted

[1] We do not analyse the scenario with an exomoon orbiting WASP-10b because no transit duration variation, predicted by Kipping (2009), was detected in our data.

Table 4. Outer-perturber solutions that reproduce the observed O − C variation. $P^{\rm ttv}$ indicates which periodicity in the O − C diagram ($P_1^{\rm ttv}$ or $P_2^{\rm ttv}$) is reproduced by a solution, $a_{\rm c}$ denotes the semimajor axis of the perturbing planet, $M_{\rm c}$ is its mass, $P_{\rm c}$ is its orbital period, $K_{\rm c}$ is the expected semi-amplitude of the RV variation and $\chi^2_{\rm red}$ is the lowest value of reduced chi-square for direct model fitting.

No.	$P^{\rm ttv}$	$a_{\rm c}$ (au)	$M_{\rm c}$ ($M_{\rm J}$)	$P_{\rm c}$ (d)	$K_{\rm c}$ (m s^{-1})	$\chi^2_{\rm red}$
1	1	0.0536	0.10	5.2293	14.2	1.5
2	2	0.0539	0.10	5.2647	14.1	2.5
3	2	0.0682	0.55	7.4962	69.1	2.8
4	1	0.0686	0.55	7.5677	68.9	2.8

to observed data by shifting along the time axis and adjusting to the time-span covered by observations. The best-fitting solutions are given in Table 4. The chi-square test favours solution 1, which reproduces $P_1^{\rm ttv}$ with minimal $\chi^2_{\rm red} = 1.5$. This value is significantly smaller than $\chi^2_{\rm red}$ obtained in an analogous way for the remaining configurations. The O − C diagram with solution 1 is presented in Fig. 6, where the residuals are also plotted.

5 SPECTROSCOPIC REANALYSIS AND STELLAR ACTIVITY

To reassess the possible solutions, we have reanalysed the radial-velocity (RV) data published by Christian et al. (2009). We used the SYSTEMIC CONSOLE software (Meschiari et al. 2009). The host star is known to be variable because of stellar rotation and star-spots (Smith et al. 2009). It has been shown that this effect may generate RV variations up to a few hundred m s^{-1} (Hatzes 2002) and mimic a planetary companion on a Keplerian orbit (Desort et al. 2007). We have reanalysed the RV data assuming that WASP-10b has a circular orbit. This has resulted in a best-fitting model with $\chi^2_{\rm red} = 3.9$ and rms $= 49.6$ m s^{-1}. The periodogram of the residuals (Fig. 7) reveals a periodicity of ∼11.84 d, a value close to the period of stellar rotation $P_{\rm rot} = 11.91 \pm 0.05$ d determined

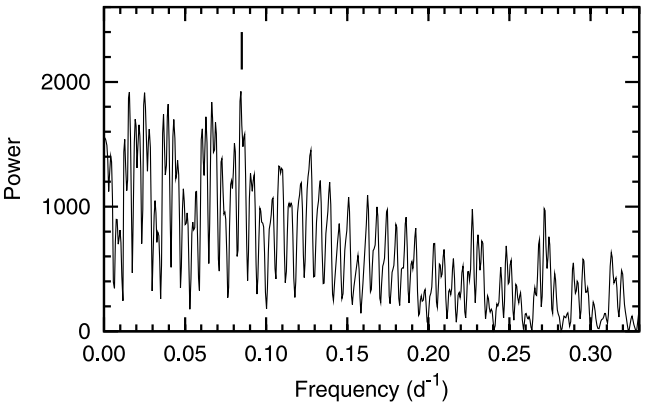

Figure 7. The Lomb–Scargle periodogram for the RV residuals after removing the transiting planet in a circular orbit. A peak corresponding to the stellar rotation is marked.

by Smith et al. (2009). The fitting procedure was repeated with an additional sinusoid signal of period $P_{\rm rot}$ and a floating phase and amplitude. The eccentricity of WASP-10b, $e_{\rm b}$, was also allowed to vary. This resulted in a significantly improved model with $\chi^2_{\rm red} = 2.5$ and rms $= 31.4$ m s^{-1}. The eccentricity was found to be $e_{\rm b} = 0.013 \pm 0.063$ and it is statistically indistinguishable from zero. Therefore, we adopted $e_{\rm b} = 0.0$ in further analysis. This result is not surprising as tidal interactions with the host star are expected to circularize the orbit of the planet (Zahn 1977).

To check whether the perturbing planet may be hidden in the RV residuals of the model composed of planet b and star-spots, a second planet with physical and orbital parameters as in solutions 1–4 was put into the system. A circular Keplerian orbit of the second planet and coplanarity were assumed for simplicity. We note that only solutions 1 and 2 significantly decrease the rms of the RV model to 24.7 and 22.5 m s^{-1}, respectively. Combining the results of the TTV and RV analyses, we have found solution 1 the most likely. The RV curves are plotted in Fig. 8 for individual components (i.e. WASP-10b, WASP-10c and the star-spot effect).

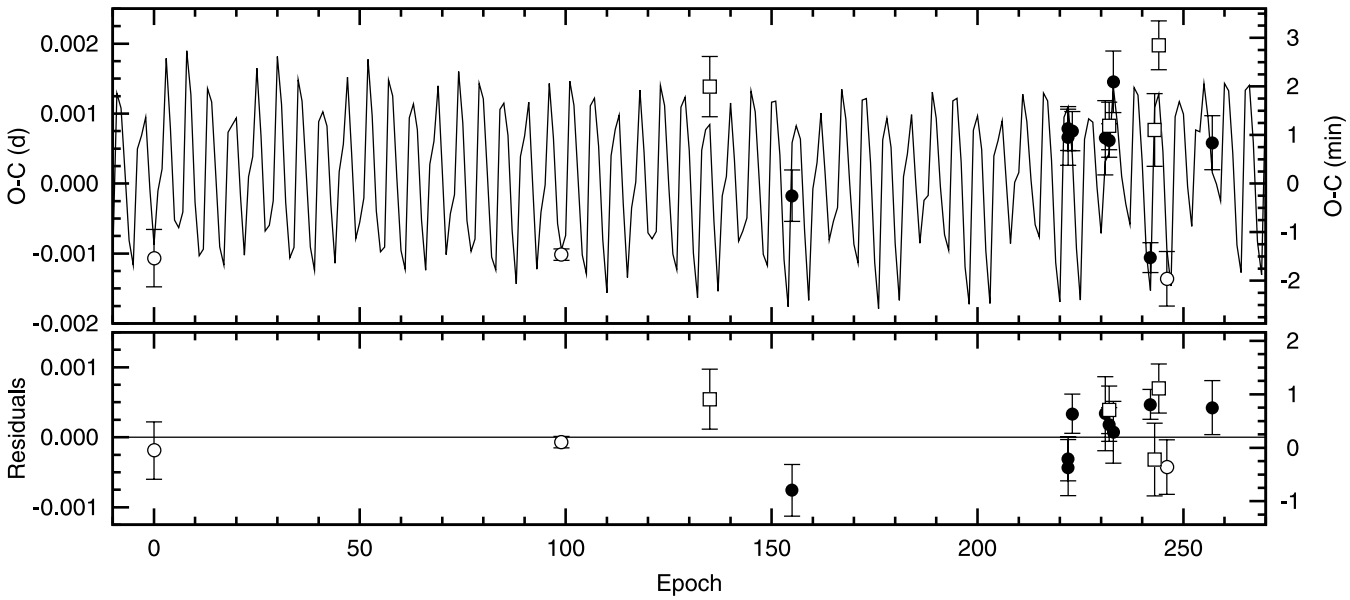

Figure 6. The O − C diagram for WASP-10b with the best-fitting model (solution 1 in Table 4). The mass of the perturber is 0.10 $M_{\rm J}$ and its orbital period is ∼5.23 d. Symbols are the same as in Fig. 2. Residuals are plotted in the bottom panel.

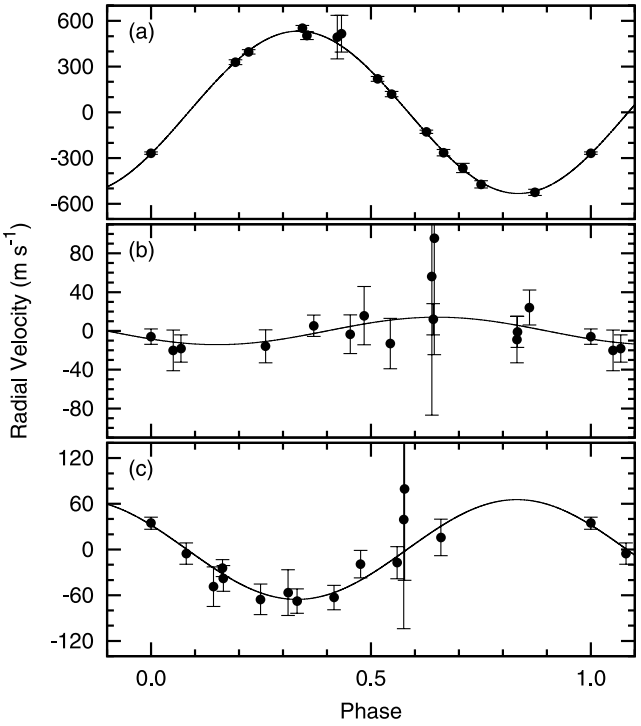

Figure 8. The RV curves after removing the remaining two components for (a) WASP-10b, (b) WASP-10c and (c) the star-spot effect. Data have been taken from Christian et al. (2009). Two points with large error bars were obtained in poor weather conditions and may exhibit systematic errors as a result of scattered moonlight (see, for example, Latham et al. 2010).

The RV semi-amplitude generated by stellar rotation was found to be $\sim$65 m s^{-1}. RV observations by Christian et al. (2009) span from 2007 August to 2008 February and are partially covered by photometric observations from the SuperWASP survey (Pollacco et al. 2006). Smith et al. (2009) determined the amplitude of photometric variation in the 2004 and 2006 seasons only. To find this variation in the 2007 season and to verify determinations from Smith et al. (2009), the analysis of variance method (ANOVA; Schwarzenberg-Czerny 1996) was applied to the WASP-10 light curve, divided into individual seasons. A periodic signal was identified. Then, a sinusoid was fitted to the phased light curve to determine the amplitude. We determined peak-to-peak amplitudes of 20.8 $\pm$ 1.3, 10.4 $\pm$ 1.0 and 8.5 $\pm$ 0.9 mmag for the 2004, 2006 and 2007 seasons, respectively. Our values are similar to the results of Smith et al. (2009), who reported 20.2 and 12.6 mmag for 2004 and 2006, respectively. Desort et al. (2007) have shown that for a G2 V-type star with $v \sin i = 7$ km s^{-1} and a photometric amplitude of 1 per cent (parameters close to those of WASP-10), a spot may produce RV variations with the semi-amplitude of $\sim$70 m s^{-1}. This estimation is consistent with the value determined by us from the RV model analysis.

Stellar spots may affect the transit depth (e.g. Czesla et al. 2009). In our data, we have found that transit depth variation is smaller than the level of 3σ for individual transits, which is thus insignificant. If stellar spots are located along a planet's path projected on to a stellar disc, the shape of the transit may be deformed. This effect may have an influence on determining mid-transit times and may result in a spurious periodic TTV signal (e.g. Alonso et al. 2009). Visual inspection of the photometric residuals (Fig. 1) does not reveal features that could be related to stellar inhomogeneities rather than to red noise. In particular, there are no deviations visible in the light-curve residuals during ingress or egress. Such deformations caused by occulting spots located close to the limb of a stellar disc are expected to generate significant TTV amplitude, even greater than a minute (Miller-Ricci et al. 2008). Furthermore, no peak close to the rotational period of the star was found in the periodogram of the O $-$ C diagram (Fig. 3) and $f_1^{\rm ttv}$ is not an alias of the rotational frequency of the host star (Alonso et al. 2009).

The proposed model of the WASP-10 system (solution 1) was found to be dynamically stable. Simulations were performed with the SYSTEMIC CONSOLE, employing the Bulirsch–Stoer integrator, and covered 10^6 yr with a maximal time-step of 10^{-4} yr. The eccentricity of WASP-10b was found to be close to zero, while the eccentricity of WASP-10c did not exceed 0.05 with a median value of 0.024.

6 AGE OF THE SYSTEM

Given the relatively short rotation period of $\sim$12 d of WASP-10, gyrochronology (Barnes 2007) can roughly yield the age of the star. For a K5 dwarf with $(B - V) = 1.15$ mag (Schmidt-Kaler 1982), we obtain 270 $\pm$ 80 Myr only, suggesting that the star (and the planetary system) is quite young. Christian et al. (2009) estimated the rotational age to be between 600 Myr and 1 Gyr, by comparing the spin period of WASP-10 to stars in Hyades (Terndrup et al. 2000). However, we must note that, according to figs 7 and 8 in Terndrup et al. (2000), there are also Pleiades members of spectral type around K5 (like WASP-10) with $v \sin i$ around 6 km s^{-1} or lower (like WASP-10; Christian et al. 2009). This method shows that it is possible for WASP-10 to have a Pleiades-like young age or an age intermediate between Pleiades and Hyades.

To confirm the relative young age of WASP-10, we have investigated its kinematic properties. The proper motion of WASP-10 is $(\mu_\alpha \cos\delta, \mu_\delta) = (21.4 \pm 2.0, -28.9 \pm 1.0)$ mas yr^{-1} (Zacharias et al. 2003) and its RV is -11.44 ± 0.03 km s^{-1} (Christian et al. 2009), yielding a heliocentric velocity of $(U, V, W) = (-0.3 \pm 0.9, -17.3 \pm 1.7, -8.1 \pm 3.2)$ km s^{-1}. First, we compared the star's spatial velocity with those of known nearby moving groups, including the Pleiades and Hyades (Antoja et al. 2008, e.g. their fig. 5 and table 3; Zhao, Zhao & Chen 2009, e.g. their fig. 2 and table 1). We have found that WASP-10 cannot be associated with any of the moving groups. In fact, it lies in an area in the U–V plane where the star density is low. This may indicate that this star was either formed in isolation (very rare) or was ejected from its parent association.

If WASP-10 was ejected recently, then it might be possible to identify its parent cluster. As stars are ejected most likely soon after cluster formation – as a result of a supernova event in a binary system (e.g. Blaauw 1961) or via dynamical interactions in a dense cluster (e.g. Poveda, Ruiz & Allen 1967) – the age of WASP-10 should be its kinematic age (i.e. it left its parent cluster some hundred Myr ago. For such a long time, it is hardly possible to reconstruct the past trajectory of the system as well as the past trajectory for a potential parent cluster because both the star and the cluster have experienced a complete cycle (or even more) around the Galactic Centre. Considering a time-span up to 1 Gyr, even periodic appearances of close encounters between the star and a cluster could occur. Moreover, it is not unlikely that WASP-10 experienced some perturbations of its path. For these reasons, the parent cluster of WASP-10 might remain unidentified if the star was ejected relatively soon after formation. If, for some reason, WASP-10 was ejected recently, finding its parent cluster could be possible. The system's peculiar spatial velocity is 10 $\pm$ 2 km s^{-1}; the heliocentric velocity was corrected for solar motion and Galactic rotation by applying the local standard of rest

Table 5. Open clusters for which close encounters with WASP-10 were found some Myr in the past. Column 1 gives the cluster designation. Columns 2 and 3 indicate the separation d between WASP-10 and the cluster centre and the radius R of the cluster. Column 4 states the time τ of the encounter (time before present) and column 5 quotes the cluster age as given in Dias et al. (2010). d was derived from three-dimensional Gaussian distributions that can explain the slope of the d distribution (see Tetzlaff et al. 2010a).

Cluster	d (pc)	R (pc)	τ (Myr)	Age (Myr)
Platais 2	0 ± 6	10	13	400
ASCC 123	0 ± 12	6	11	260

from Tetzlaff, Neuhäuser & Hohle (2010b) and a value of $V_{\odot,rot} = 225\,\mathrm{km\,s^{-1}}$. Considering a typical cluster radius of a few parsec, the parent cluster of WASP-10 can be clearly identified if the star system was ejected not earlier than some Myr ago. During 20 Myr, the star travelled about 200 pc. Taking into account the current distance to the Sun of about 100 pc and considering also previous age constraints, we selected open clusters within 300 pc from the Sun, having ages between 100 and 800 Myr (corresponding to the ages of the Pleiades and Hyades, respectively) from the Dias et al. (2010) data base for open clusters, with full kinematics available with the catalogue as well as the Hyades cluster (WEBDA;[2] Mermilliod & Paunzen 2010), 14 clusters in total. We calculated the past orbits of WASP-10 and each cluster in the Galactic potential (Harding et al. 2001) using the epicycle approximation (Lindblad 1959; Wielen 1982). Then, we performed a Monte Carlo simulation varying the distance, proper motion and RV within their confidence intervals to account for their uncertainties. The goal was to find close encounters between WASP-10 and any cluster in the past. Two clusters, for which close encounters with WASP-10 were found (within three times the cluster radius corresponding to approximately 3σ), are listed in Table 5. The cluster radius, the time of the encounter and the age of the clusters are given. If WASP-10 really originated from either Platais 2 or ASCC 123, the star is about 260–400 Myr old, in agreement with our age estimate of 270 ± 80 Myr. It is, of course, more likely that the star is ejected early in the life of a cluster. It is generally not possible to trace WASP-10 backwards reliably for the estimated age of the system.

The young age of the host star may explain the large radius of its planet, WASP-10b. The non-irradiated models by Baraffe et al. (2003), interpolated for such a young 3-M_J planet, result in a radius of $\sim$1.2 R_J. Irradiation may increase the planetary radius by $\sim$10 per cent, compared to non-irradiated models (Baraffe et al. 2003). An analogous procedure based on irradiated planetary models by Fortney, Marley & Barnes (2007) and Baraffe, Chabrier & Bartman (2008) also gives a radius of $\sim$1.2 R_J for a 300-Myr-old giant planet. This estimate is consistent with the radius of WASP-10b reported by Christian et al. (2009), Dittmann et al. (2010) and Krejcová et al. (2010).

7 CONCLUSIONS

Our investigation indicates that transit timing of WASP-10b cannot be explained by a constant period of the exoplanet. The distribution of data points in the O − C diagram reveals the existence of a periodic signal. We constructed a provisional hypothesis assuming the presence of the third body in the system. Combining the results of three-body simulations and RV measurements, the most likely explanation of the observations is given by a model with a second planet of mass of $\sim$0.1 M_J and orbital period of $\sim$5.23 d.

A reanalysis of RV data shows that WASP-10b orbits its active host star in a circular orbit. The signature of stellar rotation was found in RV measurements. This effect was misinterpreted in previous studies as a non-zero eccentricity of the transiting planet. The second planet would generate wobbling of the host star with the semi-amplitude of $\sim$14 $\mathrm{m\,s^{-1}}$, much less than the RV variation caused by the stellar rotation. Although we managed to distill this weak signal, we emphasize that further simultaneous spectroscopic and photometric observations are needed to study the activity of WASP-10 and to verify the existence of the planet WASP-10c.

WASP-10 has been found to be a relatively young star. Assuming that this finding, which is based on stellar gyrochronology, is correct, then the observed radius of WASP-10b is consistent with theoretical models and no tidal heating is required to match its radius. If planetary gas giants form by gravitational contraction, then young planets should be larger than older ones. If the planets of WASP-10 formed at larger separation than their present location, then migration must have taken place within the young age of the star.

The existence of WASP-10c could be independently confirmed if it is a transiter. Assuming that its radius is $\sim$0.4 R_J (i.e. similar to exoplanets of similar mass such as HAT-P-11b Bakos et al. 2010 or Kepler-4b Borucki et al. 2010), the expected flux drop during a transit would be $\sim$0.3 per cent or even greater if we consider the young age of the system. This could be observable with a large ground-based telescope.

In the proposed model, the ratio of orbital periods of the planets $P_c/P_b = 1.69$ is very close to the 5 : 3 orbital resonance. A significant fraction of known multiplanet systems are in MMRs, mainly in low-order ones. Two planets in wide orbits and trapped in a 3 : 2 MMR were found around HD 45364 by RV measurements (Correia et al. 2009). Planets in the four-planetary system around GJ 581 (Mayor et al. 2009) are very close to 5 : 2 (GJ 581b and c) and 5 : 3 (GJ 581e and b) MMRs (Papaloizou & Terquem 2010). Therefore, we conclude that the architecture of the WASP-10 system would not be completely unusual.

ACKNOWLEDGMENTS

We are grateful to the anonymous referee for remarks and for inspiring us to study the kinematic membership. We thank J. Dittmann for providing the original photometric data. We also thank G. Nowak and T. Eisenbeiss for discussions about stellar spots and gyrochronology. GM acknowledges support from the European Union in the FP6 MC ToK project MTKD-CT-2006-042514. DD acknowledges support from the project DO 02-362 of the Bulgarian Scientific Foundation. RN would like to acknowledge general support from the Deutsche Forschungsgemeinschaft (DFG). GM, RN and AN acknowledge support from the German Academic Exchange Service (DAAD) PPP–MNiSW project 50724260–2010/20011 'Eclipsing binaries in young clusters and planet transit time variations'. AN was also supported by the Polish Ministry of Science and Higher Education grant NN 203 510938. NT acknowledges financial support from Carl-Zeiss-Stiftung. SR and CM acknowledge support from the DFG in programmes NE 515/32-1 and SCHR 665/7-1, respectively. TK, JB and VK acknowledge support from the Marie Curie International Reintegration Grant FP7-200297, grant GA ČR GD205/08/H005, the National Scholarship Programme of the Slovak Republic and partly from VEGA 2/0078/10 and VEGA 2/0074/09. A part of this

[2] http://www.univie.ac.at/webda/webda.html

paper is the result of a Polish and Bulgarian Academies of Sciences (PAN/BAN) exchange and a joint research project 'spectral and photometric studies of variable stars'. We have used the Exoplanet Transit Data base (http://var.astro.cz/ETD) and data from the Wide Angle Search for Planets (WASP) public archive in this research. The WASP consortium comprises the University of Cambridge, Keele University, University of Leicester, The Open University, The Queen's University Belfast, St Andrews University and the Isaac Newton Group. Funding for WASP comes from the consortium universities and from the UK's Science and Technology Facilities Council.

REFERENCES

Agol E., Steffen J., Sari R., Clarkson W., 2005, MNRAS, 359, 567
Alonso R., Aigrain S., Pont F., Mazeh T., CoRoT Exoplanet Science Team, 2009, in Pont F. et al., eds, Proc. IAU Symp. 253, Transiting Planets. Kluwer, Dordrecht, p. 91
Anglada-Escude G., López-Morales M., Chambers J. E., 2010, ApJ, 709, 168
Antoja T., Figueras F., Fernández D., Torra J., 2008, A&A, 490, 135
Bakos G. Á. et al., 2010, ApJ, 710, 1724
Baraffe I., Chabrier G., Bartman T. S., Allard F., Hauschildt P. H., 2003, A&A, 402, 701
Baraffe I., Chabrier G., Bartman T. S., 2008, A&A, 482, 315
Barnes S. A., 2007, ApJ, 669, 1167
Blaauw A., 1961, Bull. Astron. Inst. Netherlands, 15, 265
Borucki W. J. et al., 2010, ApJ, 713, 126
Chambers J. E., 1999, MNRAS, 304, 793
Christian D. J. et al., 2009, MNRAS, 392, 1585
Correia A. C. M. et al., 2009, A&A, 496, 521
Czesla A., Huber K. F., Wolter U., Schröter S., Schmitt J. H. M. M., 2009, A&A, 505, 1277
Dias W. S., Alessi B. S., Moitinho A., Lepine J. R. D., 2010, Optically visible open clusters and Candidates, VizieR On-line Data Catalogue, B/ocl (originally published in 2002, A&A, 389, 871)
Dittmann J. A., Close L. M., Scuderi L. J., Morris M. D., 2010, ApJ, 717, 235
Desort M., Lagrange A.-M., Galland F., Udry S., Mayor M., 2007, A&A, 473, 983
Eastman J., Siverd R., Gaudi B. S., 2010, PASP, 122, 935
Everett M. E., Howell S. B., 2001, PASP, 113, 1428
Fortney J. J., Marley M. S., Barnes J. W., 2007, ApJ, 659, 1661
Gibson N. P. et al., 2009, ApJ, 700, 1078
Hatzes A. P., 2002, Astron. Notes, 323, 392
Harding P., Morrison H. L., Olszewski E. W., Arabadjis J., Mateo M., Dohm-Palmer R. C., Freeman K. C., Norris J. E., 2001, AJ, 122, 1397
Holman M. J., Murray N. W., 2005, Sci, 307, 1288
Johnson J. A., Winn J. N., Cabrera N. E., Carter J. A., 2009, ApJ, 692, L100
Johnson J. A., Winn J. N., Cabrera N. E., Carter J. A., 2010, ApJ, 712, L122
Kipping D. M., 2009, MNRAS, 392, 181
Kipping D. M., Bakos G. Á., 2010a, preprint (astro-ph/1004.3538)
Kipping D. M., Bakos G. Á., 2010b, preprint (astro-ph/1006.5680)
Krejcová T., Budaj J., Krushevska V., 2010, preprint (astro-ph/1003.1301)
Latham D. W. et al., 2010, ApJ, 713, L140
Lendl M., Afonso C., Koppenhoefer J., Nikolov N., Henning Th., Swain M., Greiner J., 2010, A&A, 522, 29
Lindblad B., 1959, Handbuch der Physik, Vol. 53. Springer, Berlin, p. 21
Lomb N. R., 1976, Ap&SS, 39, 447
Maciejewski G. et al., 2010, MNRAS, 407, 2625
Mandel K., Agol E., 2002, ApJ, 580, 171
Mayor M. et al., 2009, A&A, 507, 487
Mermilliod J.-C., Paunzen E., 2003, A&A, 410, 511
Meschiari S., Wolf A. S., Rivera E., Laughlin G., Vogt S., Butler P., 2009, PASP, 121, 1016
Miller-Ricci E. et al., 2008, ApJ, 682, 593
Miralda-Escudé J., 2002, ApJ, 564, 1019
Mugrauer M., Berthold T., 2010, Astron. Notes, 331, 449
Nesvorný D., Morbidelli A., 2008, ApJ, 688, 636
Nesvorný D., 2009, ApJ, 701, 1116
Niedzielski A., Maciejewski G., Czart K., 2003, Acta Astron., 53, 281
Papaloizou J. C. B., Terquem C., 2010, MNRAS, 405, 573
Poddaný S., Brát L., Pejcha O., 2010, New Astron., 15, 297
Pollacco D. et al., 2006, PASP, 118, 1407
Poveda A., Ruiz J., Allen C., 1967, Boletin de los Observatorios Tonantzintla y Tacubaya, 4, 86
Scargle J. D., 1982, ApJ, 263, 835
Schmidt-Kaler T., 1982, in Schaifers K., Voigt H. H., Landolt H., eds, Landolt-Bornstein: Numerical Data and Functional Relationships in Science and Technology. Springer, Berlin, p. 19
Smith A. M. S. et al., 2009, MNRAS, 398, 1827
Schneider J., 2004, in Favata F., Aigrain S., Wilson A., eds, Second Eddington Workshop: Stellar Structure and Habitable Planet Finding, ESA SP-538. ESA Publications, Noordwijk, p. 407
Steffen J. H., Gaudi B. S., Ford E. B., Agol E., Holman M. J., 2007, preprint (astro-ph/0704.0632)
Schwarzenberg-Czerny A., 1996, ApJ, 460, 107
Terndrup D. M., Stauffer J. R., Pinsonneault M. H., Sills A., Yuan Y., Jones B. F., Fischer D., Krishnamurthi A., 2000, AJ, 119, 1303
Tetzlaff N., Neuhäuser R., Hohle M. M., Maciejewski G., 2010a, MNRAS, 402, 2369
Tetzlaff N., Neuhäuser R., Hohle M. M., 2010b, MNRAS, in press (doi:10.1111/j.1365-2966.2010.17434.x)
Van Hamme W., 1993, AJ, 106, 2096
Wielen R., 1982, in Landolt-Börnstein, Group VI/2c, Astronomy and Astrophysics. Springer, Berlin, p. 208
Zacharias N., Urban S. E., Zacharias M. I., Wycoff G. L., Hall D. M., Germain M. E., Holdenried E. R., Winter L., 2003, The 2nd US Naval Observatory CCD Astrograph Catalog (UCAC2)
Zahn J.-P., 1977, A&A, 57, 283
Zhao J., Zhao G., Chen Y., 2009, ApJ, 692, 113

This paper has been typeset from a TEX/LATEX file prepared by the author.